

## Supplementary Materials for

### **Impact of nuclear vibrations on van der Waals and Casimir interactions at zero and finite temperature**

Prashanth S. Venkataram\*, Jan Hermann, Teerit J. Vongkovit, Alexandre Tkatchenko, Alejandro W. Rodriguez

\*Corresponding author. Email: psv2@princeton.edu

Published 1 November 2019, *Sci. Adv.* **5**, eaaw0456 (2019)

DOI: 10.1126/sciadv.aaw0456

#### **This PDF file includes:**

Section S1. VDW interaction free energies

Section S2. VDW interactions of one versus two carbyne wires

Section S3. DFT phonon dispersions for carbyne and graphene

Section S4. RPA model of doped graphene

Section S5. VDW power laws versus dimensionality for perfect conductors

Fig. S1. vdW free energies of low-dimensional compact molecules.

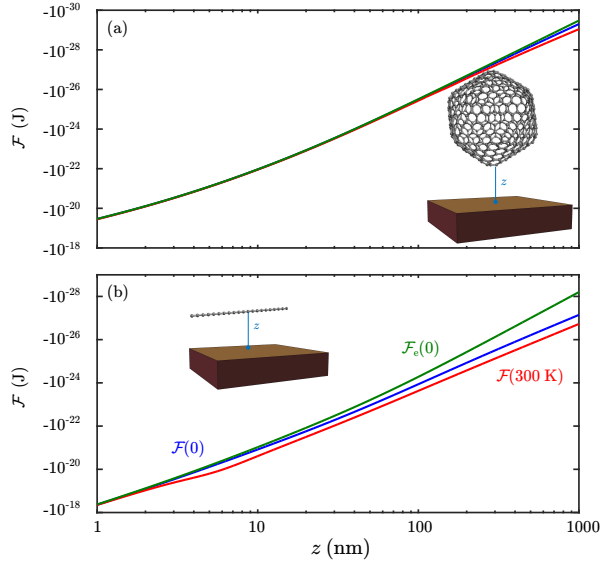
Fig. S2. vdW free energies of two-dimensional materials.

Fig. S3. Nonmonotonicity and temperature deviations due to phonon-induced nonlocal response in carbyne at short distance from the gold plate.

Fig. S4. Phonon dispersions of carbyne and graphene.

Fig. S5. Graphene interaction power laws in the continuum RPA model.

Table S1. Power laws versus dimensionality for perfect conductors.



**Fig. S1. vdW free energies of low-dimensional compact molecules.** vdW interaction free energies of (a) a fullerene or (b) a carbyne wire, each with a gold plate, comparing results with phonons at zero (blue) or room (red) temperatures with those without phonons (green).

### Section S1. VDW interaction free energies

Having presented the power laws of the vdW interaction free energies in the main text, we now present the free energies themselves for the systems considered.

For the compact molecular systems of fullerene [Fig. 1(a)] or a carbyne wire [Fig. 1(b)], we find free energies that do not exceed  $10^{-18}$  J in magnitude. However, for carbyne at room temperature, the nonmonotonic power law at small separation ensures that the force on the wire due to the gold plate may exceed  $10^{-11}$  N, which may be measurable, though this would require a way to stably suspend a long carbyne wire in vacuum; this is contrast to the fullerene, whose monotonic power laws and small size ensure that forces are too small to feasibly measure.

For infinite pristine graphene above a gold plate [Fig. 2(a)], we find that the RMB free energies (per unit area) at zero and room temperature coincide at small separation but diverge from each other at larger separations. This is in contrast to the RPA free energies at zero versus room temperature, which never coincide with each other. This is a reflection of the abil-

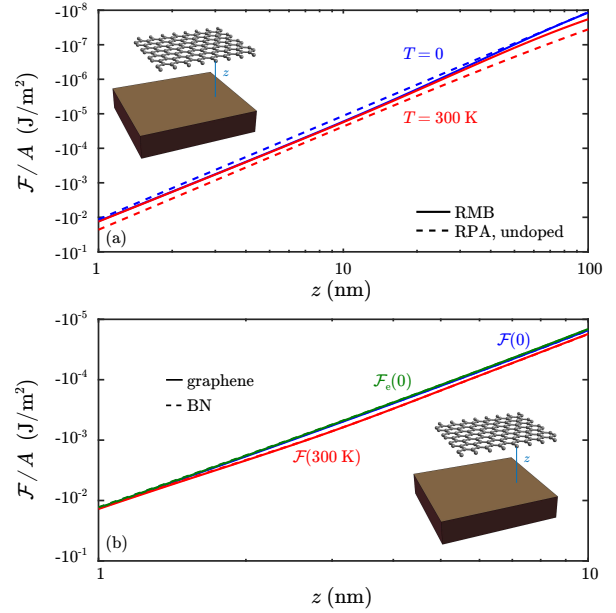


**Fig. S2. vdW free energies of two-dimensional materials.** (a) vdW interaction free energies per unit area of an infinite sheet of pristine graphene with a gold plate, comparing RMB (solid) and RPA (dashed) results at zero (blue) or room (red) temperatures. (b) vdW interaction free energies per unit area of supercells of graphene (solid) or BN (dashed) of approximate size  $11 \text{ nm} \times 10 \text{ nm}$ , comparing results with phonons at zero (blue) or room (red) temperatures with those without phonons (green).

ity of the material model for graphene in the RPA framework to capture intrinsic finite temperature effects like excitation of electrons away from the Dirac point, whereas the material model used in the RMB framework is computed only at zero temperature, and only the effects of temperature on long-range EM interactions via the Matsubara summation are directly captured. Additionally, the RMB power law at zero temperature decreases and then increases again for  $z > 10$  nm, which is why the RMB free energy at zero temperature eventually approaches the RPA free energy at zero temperature; no such coincidence is observed for the RMB and RPA free energies at room temperature.

For pristine graphene or BN supercells above a gold plate [Fig. 2(b)], we see insignificant differences in the RMB free energies (per unit area), evinced by the overlapping lines for the corresponding cases in each system. Additionally, the room temperature power laws for both graphene and BN su-

percells show bumps around  $z \approx 3$  nm, reflecting the non-monotonicity of the corresponding power laws at those separations. This is similar to the case of carbyne, but different from infinite graphene. It is worth noting that at  $z = 1$  nm, the free energies for the graphene supercell are larger than their counterparts for infinite graphene by 1.5% and 3.8% at zero and room temperatures, respectively; these suggest convergence of the finite supercells to the infinite results at such small separations. By contrast, at  $z = 10$  nm, these free energies for the graphene supercell are *smaller* than their counterparts for infinite graphene by 10.6% at zero temperature and 0.4% at room temperature. The separation  $z = 10$  nm is large enough for the finite size of the supercell to become relevant, and the deviations at zero temperature free energies reflects this. The much smaller deviation in the room temperature free energies at this separation is because the room temperature power law for the supercell exhibits nonmonotonic behavior for  $z < 10$  nm due to the confluence of material effects, low dimensionality, and finite size, whereas this does not occur for infinite graphene at room temperature, demonstrating qualitative divergence of the supercell behavior from that of infinite graphene at room temperature for larger separations.

## Section S2. vdW interactions of one versus two carbyne wires

We expand on the issue of nonmonotonic vdW interaction power laws at finite temperature between carbyne and a gold plate, specifically regarding whether this is an artifact of the overlap of enlarged Gaussian basis functions with the plate. Strictly speaking, for a wire parallel to a conducting plane, modeling the latter via a local macroscopic susceptibility becomes questionable for  $z < \sigma_0(0)$ , as we expect the atomism and spatially dispersive response of the latter to matter more for such small separations. Such an issue is not relevant when considering interactions between two molecules in vacuum. We further explore this by comparing the RMB interaction power laws (in the presence of phonons) of a single carbyne wire above the gold plate, equivalent to a wire interacting with its correlated image, against that of two parallel, uncorrelated wires interacting in vacuum. In particular, we study wires comprising either 250, 500, or 1000 atoms at zero [Fig. 3(d)] and room [Fig. 3(e)] temperatures. At zero temperature, the power laws for a single wire above the plate are all monotonic even at small  $z$ , because the free energy is not sensitive to the nonmonotonic integrand for  $z < \sigma_0(0)$ ; essentially, the wire is interacting with its correlated image, which dramatically changes the phonon polaritons emerging from the long-range EM couplings, compared to those of the wire in vacuum. In contrast, the power laws for two wires of at least 500 atoms in vacuum show nonmonotonicity for  $z > 10$  nm, which is larger than  $\sigma_0(0)$  and hence cannot be attributed to overlapping Gaussian basis functions. At room temperature, the power laws for a single wire above the plate show nonmonotonicity only for  $z$  not much greater than  $\sigma_0(0)$

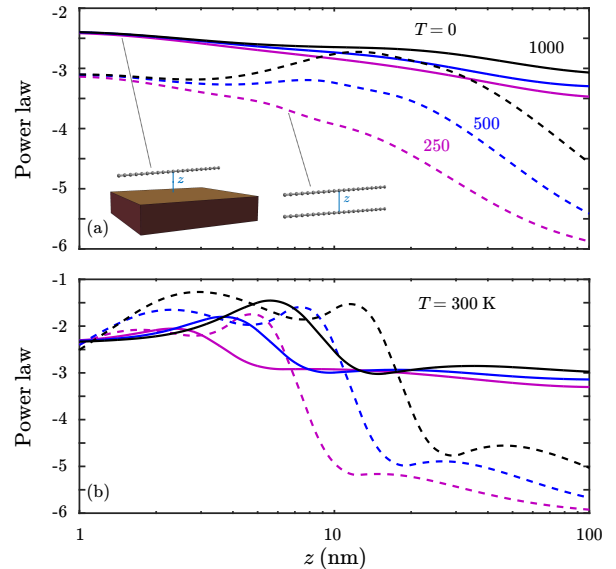


**Fig. S3. Nonmonotonicity and temperature deviations due to phonon-induced nonlocal response in carbyne at short distance from the gold plate.** Power laws for the vdW interactions of one parallel carbyne wire with a gold plate (solid) or two such wires in vacuum (dashed) for wires made of 250 (magenta), 500 (blue), or 1000 (black) atoms, at  $T = 0$  (a) or  $T = 300$  K (b).

for every wire length, while the power laws for two wires in vacuum show two maxima for  $z < 20$  nm, with the maxima at larger  $z$  corresponding to the aforementioned maxima visible for two wires even at zero temperature and occurring in the absence of overlapping Gaussian widths. Thus, it is clear that as nonmonotonic vdW interaction power laws can be observed at room temperature for separations both on the order or larger than the corresponding Gaussian smearing widths, and is therefore not an artifact of overlapping response functions or the lack of atomism in our description of the plate.

## Section S3. DFT phonon dispersions for carbyne and graphene

The internuclear couplings  $K_I$  that enter the response  $\mathbb{V}$  of every molecular system we test are derived from density functional theory (DFT) calculations in the following way. Under the Born–Oppenheimer approximation, we find the electron density minimizing the electronic energy for a fixed set of nuclear coordinates, and iteratively vary the nuclear coordinates until the total energy is minimized to determine the ground state (relaxed) structure. This is done with periodic boundary conditions enforced particularly for carbyne and graphene. We retain only nearest neighbor internuclear couplings in graphene and second-nearest neighbor couplings in carbyne and solve  $K_I x_I = \omega^2 M_I x_I$  for the two atom basis with periodic boundary conditions, producing the phonon dispersions for graphene and carbyne in Fig. 4. The graphene phonon dispersion generally agrees well with prior theoretical

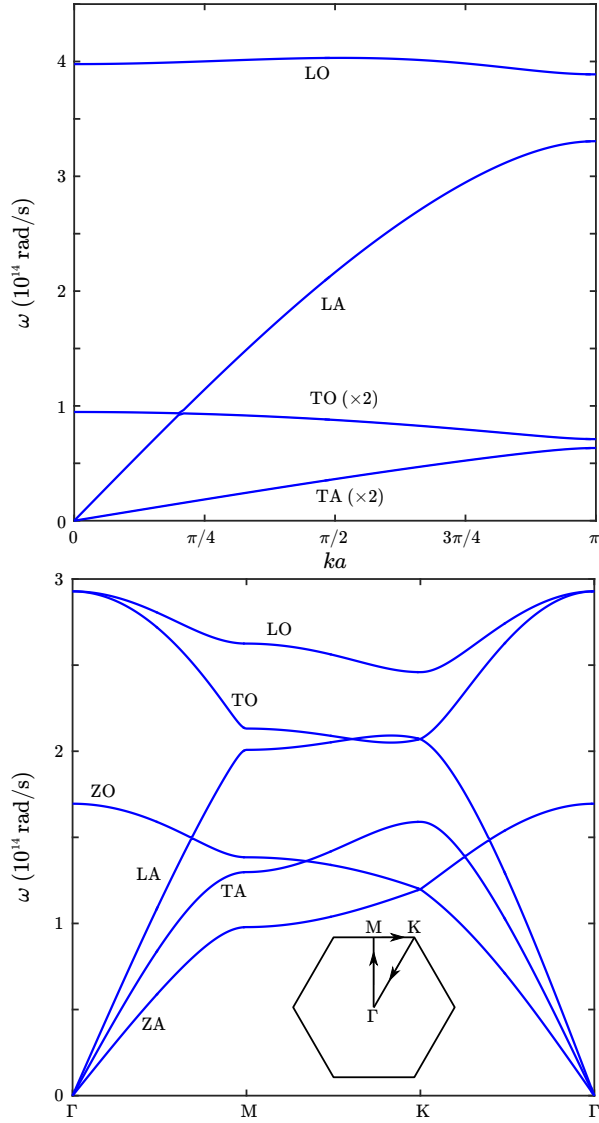


**Fig. S4. Phonon dispersions of carbyne and graphene.** The bands are computed along the Brillouin zone edge using internuclear couplings derived from density functional theory. Top: All 4 distinct bands, namely the longitudinal (L) and transverse (T) acoustic (A) and optical (O) bands for carbyne; both TA and TO bands are doubly degenerate (denoted  $\times 2$ ). Bottom: All 6 bands for graphene, distinguishing in-plane transverse (T) and out-of-plane transverse (Z) bands which are no longer degenerate.

and experimental work [Refs. 19–22 in main text], and the carbyne phonon dispersion generally agrees well with prior theoretical work [Refs. 23–25 in main text] (though experimental results for carbyne are lacking) [Fig. 4]; in any case, the exact values of the phonon frequencies, especially for optical branches at higher frequencies, are less relevant to van der Waals (vdW) interactions, where Wick rotation to imaginary frequency ensures that as the separation increases, the behavior at low frequency and long wavelength matters most when determining interaction power law behaviors.

At low frequency and long wavelength, while our model

does correctly predict the linear dispersions and associated group velocities of the longitudinal (and in-plane transverse for graphene) acoustic phonon modes, it predicts linear dispersion for the out-of-plane transverse acoustic (ZA) mode, which differs from prior predictions of quadratic dispersion of the ZA mode as  $|\mathbf{k}| \rightarrow 0$ . This is because in both atomistic and continuum treatments of mechanical deformations in carbyne and graphene [Refs. 19, 25–29 in main text], nontrivial out-of-plane internuclear couplings must be present to at least fourth-nearest neighbors (which is equivalent to the requirement that coefficients of spatial derivatives higher than first-order must be present in the continuum case) for quadratic dispersion to be present, whereas our calculations and others which only account for couplings to nearest or second-nearest neighbors will fail to capture this; in both carbyne and graphene, our model does not show significant changes to the dispersion in the limit  $|\mathbf{k}| \rightarrow 0$  when second-nearest neighbor couplings are accounted for compared to accounting for only nearest neighbors, while we were unable to attain an adequate relative convergence for third- and higher-nearest neighbors in our DFT calculations of carbyne and graphene, though we stress that as  $K_I$  can in principle encode couplings between arbitrary pairs of nuclei, this is a problem with our particular computations, not a drawback of the RMB method itself. The linear versus quadratic behavior is a significant difference given the sensitive dependence of vdW interactions to response properties at low frequency and long wavelength: a linear acoustic phonon branch would have a phonon density of states (DOS) that in the limit  $|\mathbf{k}| \rightarrow 0$  respectively approaches a nonzero constant in 1 spatial dimension or vanishes linearly with frequency as in 2 spatial dimensions, while a quadratic branch would respectively have a square root singularity or have a nonzero constant phonon DOS in the corresponding limits, so our model underestimates the contribution of ZA phonon modes to the delocalized response and to vdW interaction power laws in turn. Despite these deficiencies, we use values of  $K_I$  obtained from our DFT calculations rather than empirically fitted parameters for specific subsystems so that we may have a consistent comparison of results obtained for compact molecules like fullerenes. Moreover, for the specific case of graphene, our use of nuclear damping coefficients  $B_I$  corresponding to relaxation rates  $\gamma_I = 10^{13}$  rad/s will smear out the details of the phonon dispersion for  $\omega < \gamma_I$ , making those particular details less relevant for qualitative or quantitative prediction of vdW interactions.

We point out that the need for higher-nearest neighbor couplings to accurately capture the quadratic dispersion of out-of-plane acoustic phonon modes in the limit  $|\mathbf{k}| \rightarrow 0$  in extended low-dimensional carbon allotropes is indirectly indicative of Dobson type-C nonadditivity, namely the inherent quantum delocalization of electronic states. In particular, while such delocalization will change the details of the electronic response at high frequencies, such high-frequency resonant behavior is less relevant to vdW interactions at the mesoscopic scale of tens of nanometers. By contrast, if such delocalized electron states interact with coupled nuclear degrees of

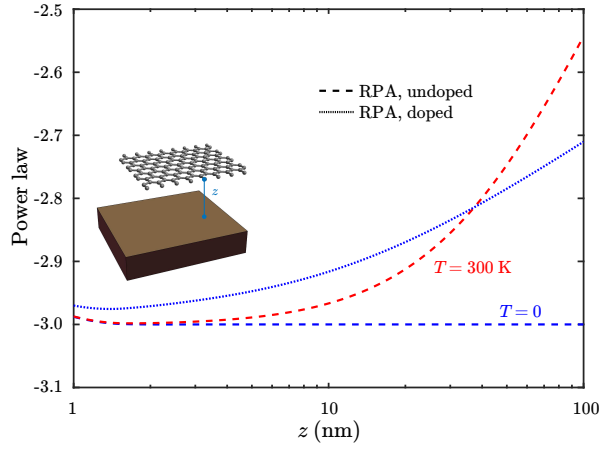


**Fig. S5. Graphene interaction power laws in the continuum RPA model.** Power laws for the vdW interactions of parallel infinite graphene with a gold plate, at zero (blue) or room (red) temperatures with (fine dashed) or without (coarse dashed) doping. The doping density is  $10^{13} \text{ cm}^{-2}$ .

freedom over longer length scales, thereby mediating internuclear interactions that may be nontrivial even at the level of fourth-nearest neighbors, the resulting qualitative changes to the phonon dispersion at low frequency in the limit  $|\mathbf{k}| \rightarrow 0$  will likely have a much more dramatic impact on vdW interactions at the mesoscale, particularly at finite temperature. Once again, we emphasize that the RMB method can account for higher-nearest neighbor couplings as long as properly converged data can be provided when constructing  $K_I$ , but we leave the resolution of such details to future work.

#### Section S4. RPA model of doped graphene

We compare the vdW interaction power laws for the RPA model of graphene above a gold plate at zero or room temperature, with or without electronic doping [Fig. 5]; the doping density is  $10^{13} \text{ cm}^{-2}$ . With this concentration of dopants, the electronic response is dominated by the free charge carriers particularly at small frequency and long wavelength. As a re-

sult, the power law with doping is less negative than without, and approaches the behavior of a typical metal. It is interesting to note that while the undoped power law remains a constant -3 for all  $z$ , the doped power law increases (becomes less negative) as  $z$  increases; this is in contrast to typical Casimir energy power laws which become more negative as separations increase to make retardation more relevant, though the doped power law does return to -3 for  $z \gtrsim 10 \mu\text{m}$ .

#### Section S5. VDW power laws versus dimensionality for perfect conductors

Table S1 shows the expected power law dependence of the vdW interaction free energy for a 0-dimensional dipole,

**Table S1. Power laws versus dimensionality for perfect conductors.** vdW interaction free energy power laws, in the limits  $T \rightarrow 0$  and  $T \rightarrow \infty$ , for a 0-dimensional dipole, 1-dimensional perfectly conducting wire (whose radius is much smaller than the separation), or 2-dimensional perfectly conducting plate, each parallel to a perfectly conducting plate at separation  $z$ .

Dimensionality	$T \rightarrow 0$	$T \rightarrow \infty$
0	$\frac{1}{z^4}$	$\frac{1}{z^3}$
1	$\frac{1}{z^2 \ln(z)}$	$\frac{1}{z^4}$
2	$\frac{1}{z^3}$	$\frac{1}{z^2}$

a 1-dimensional perfectly conducting thin wire, or a 2-dimensional perfectly conducting plate, each at separation  $z$  parallel to a perfectly conducting plate, in the limits  $T \rightarrow 0$  or  $T \rightarrow \infty$  [Refs. 30–31 in main text]. Note that the  $T \rightarrow \infty$  is effectively the classical thermodynamic limit where quantum fluctuations become irrelevant. We point out that the fullerene follows the 0-dimensional behavior above a perfect conducting plate. While we are unable to probe sufficiently large separations or wire lengths to test this, we expect an infinitely long carbyne wire to asymptotically behave like a 1-dimensional perfectly conducting thin wire. Finally, graphene and hexagonal BN are not perfect conductors despite the unusual Dirac cone electronic structure of graphene, so we do not expect their power laws to behave like those of perfectly conducting plates.